# Investigating Stress Transfer and Failure Mechanisms in Graphene Oxide-Cellulose Nanocrystals Films

# GEHAN JAYATILAKA, MOHAMMAD MOEIN MOHAMMADI and MEHRAN TEHRANI

#### **ABSTRACT**

Graphene oxide (GO) films have great potential for aerospace, electronics, and renewable energy applications. GO sheets are low-cost and water-soluble and retain some of Graphene's exceptional properties once reduced. GO or reduced GO (rGO) sheets within a film interact with each other via secondary bonds and cross-linkers. These interfacial interactions include non-covalent bonds such as hydrogen bonding, ionic bonding, and  $\pi$ - $\pi$  stacking. Stress transfer and failure mechanisms in GO and rGO films, specifically how linkers affect them, are not well understood. The present study investigates the influence of inter-particle interactions and film structures, focusing on hydrogen bonds introduced via cellulose nanocrystals (CNC), on failure and stress-transfer of the GO and rGO films. To this end, GO films with CNC crosslinkers were made, followed by a chemical reduction. The few-micron thick films were characterized using tensile testing. All tested films exhibited a brittle failure and achieved tensile strengths and modulus in the ~40-85 MPa and ~3.5-9 GPa ranges, respectively. To reveal stress transfer mechanisms in each sample, tensile in-situ Raman spectroscopy testing was carried out. By monitoring the changes in bandwidth and position of Raman bands while stretching the film, useful information such as sheet slippage and cross-linker interactions were gathered. The addition of CNC enhanced modulus but degraded strength for both GO and rGO films. Interestingly, the Raman G-peak shift at failure, indicative of stress transfer to individual GO/rGO particles, is commensurate with the films' strengths. Correlating these results with the structure and composition of different films reveals new understanding of stress transfer between GO/rGO particles, paving the way for the scalable manufacturing of strong and stiff GO-based films.

Gehan Jayatilaka, Walker Department of Mechanical Engineering, The University of Texas at Austin, Austin, Texas 78712, United States.

#### INTRODUCTION

Graphene-based materials have garnered much attention due to their outstanding electrical and mechanical properties. Graphene films possess many exceptional material properties, including high strength, ductility, and electrical/thermal conductivity [1]. Although these characteristics are highly desired in aerospace, electronics, and renewable energy applications, manufacturing graphene structures is difficult and costly [2].

Alternatively, graphene oxide (GO) films are produced directly from graphite and are relatively inexpensive and easy to produce [1]. Although GO exhibits some attributes of graphene, its intrinsic strength is substantially lower and is not electrically conductive [1, 3]. For graphene-based materials to be used in many electronic and energy applications, the material must be highly conductive [4]. An interesting feature of graphene oxide is its ability to have its conductivity restored through a process called reduction, which forms reduced graphene oxide (rGO).

Reduction of graphene oxide films brings the properties of the film closer to pristine graphene [4]. Reduction, chemical or thermal, is the process of removing some of the oxygen-containing functional groups (carboxyl-, epoxide-, and hydroxyl-) on the surface of GO [5]. Chemical reduction of GO should theoretically increase the electrical conductivity while also increasing the strength and ductility of the GO [2]. GO film reduction is also usually accompanied by microstructural changes and particle-particle stacking.

GO and rGO films are comprised of GO and rGO sheets, respectively, and are held together by Van der Waals forces [6]. These forces greatly affect the properties of these films. Cross-linking of hydrogen bonds has the potential to improve properties of the films [7]. One way to form hydrogen bonds is adding cellulose nanocrystals (CNC) to GO or rGO films. This is usually achieved by adding CNC to the GO solution, followed by vacuum filtration (GO-CNC). Subsequently, if a reduction step is carried out, rGO-CNC is obtained. The interfacial interactions induced by the hydrogen bonding changes how stress is transferred in the films [8].

Our current knowledge of the micro- and nano- mechanics of GO and rGO films is limited. This study uses tensile testing and in-situ Raman spectroscopy to reveal the mechanisms that affect the tensile properties of GO and rGO films. In-situ Raman spectroscopy is conducted at different. Namely, the position of the G-band and its downshift provides useful information on the cross-linker interactions with GO or rGO particles [9, 10].

## **EXPERIMENTAL**

#### **Sample Preparation**

Graphene oxide dispersed in water with a concentration of 4 mg/mL was purchased from Sigma-Aldrich and used to make the GO films. CNC (Celluforce) dispersed in water with a concentration of 10 mg/mL was used to make the GO-CNC samples. Two different precursor solutions were made, one with the GO solution and another with GO solution mixed with CNC. The GO/CNC solution was made with a mass ratio of 3:1, respectively. Both solutions were diluted with deionized (DI) water until the solution reached a concentration of 1 mg/mL. Each GO film was made with

20 mL of their respective solution. The films were fabricated using a vacuum filtration system. Each film had a diameter of about 45 mm and was tens of microns thick.

Four films were fabricated, one pure GO film and one GO/CNC film were reduced with 57% hydroiodic (HI) acid (Sigma-Aldrich). These films were submerged in the hydroiodic solution for 12 hours at room temperature and were washed with ethanol three times to remove residual HI acid and naturally dried overnight. The process to make the rGO film is schematically shown in figure 1.

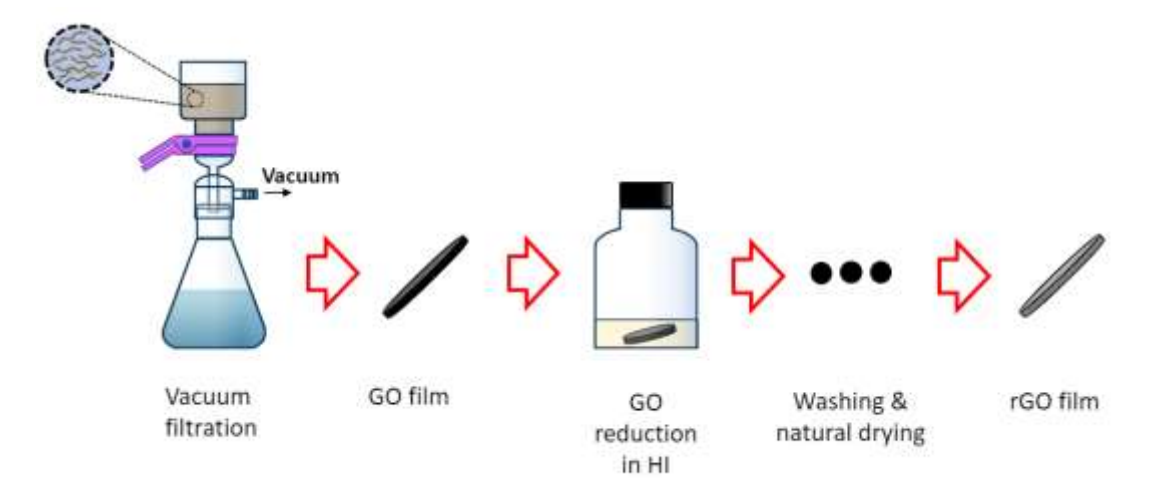


Figure 1. Schematic of the GO film fabrication process.

#### Mechanical Characterization, in-situ Raman, and Microscopy

Three rectangular strips of 3.5 mm wide and 20 mm long were cut from each film. Tensile properties of the samples were measured using a Linkam Modular Force Stage. The gap between the grips was 15 mm and the speed at which the sample was elongated was 5  $\mu$ m/s. Stress-strain curves were plotted for strip and the tensile strengths, moduli, and strains at failure were extrapolated from the graphs.

Cross-sectional samples of the four films were characterized by a Quanta scanning electron microscope (SEM). All SEM images were taken using an accelerating voltage of 30 kilovolts and at a working distance of about 10 mm.

Samples were tested in a Witec Raman Spectrometer using a 532 nm laser. Insitu Raman spectroscopy was conducted by varying strain using a Linkam Modular Force Stage under the Raman laser. Raman spectra were taken for each sample at 25  $\mu$ m intervals, starting at no strain and ending with an extension of 75  $\mu$ m. Each spectrum was taken over a slow time series of 50 measurements lasting 2 seconds each. Each measurement had 2 accumulations of spectra over 1 second.

## **RESULTS AND DISCUSSIONS**

In figure 2, tensile properties and representative stress-strain curves of the tested films are displayed. The average tensile strength for these films ranged from about 40 to 85 MPa. Their failure strains ranged from about 0.5 to 3% and their tensile moduli from 3.5 to 9 GPa. These results show how reduction and cross-linkers affect the mechanical properties of the GO films. Interpreting these results should consider

film structure, functional groups on their constituent GO and rGO particles, and cross-linkers used.

The addition of CNC increased the elastic modulus of both GO and rGO films. This effect was more pronounced for the GO films due to the abundant hydroxyl (-OH) groups on GO particles that readily participate in hydrogen bonding. Although the films with CNC have stronger inter-particle interactions, evident by their higher moduli, they do not show higher strengths when compared to their respective pure GO and rGO counterparts. Strength of all films are relatively similar, except for rGO that is clearly stronger. Similarly, representative stress-strain curves for all samples, except rGO, exhibit a linear region, up to 0.2-0.3% strain, followed by a lower slope region that is indicative of damage and possibly delamination. rGO film exhibits a linear behavior up to failure.

Strength of individual GO or rGO particles is two orders of magnitude higher than their films, indicating an inefficient utilization of their strength. Failure in GObased films starts with inter-particle slippage followed by delamination/crack formation. Packed GO or rGO particles with strong inter-particle interactions, therefore, achieve high strengths. Thickness of GO, rGO, GO-CNC, and rGO-CNC films were measured as ~18, 10, 22, and 23 µm. GO reduction is accompanied by a 44% reduction in thickness, as reduced particles pack more tightly. rGO films, therefore, exhibited the highest tensile strength. CNC increases GO film thickness by 22%, and even HI reduction doesn't improve packing of particles in rGO-CNC films. Comparing all results, it is apparent that the reduction process improved ductility and tensile strength or rGO films only. This phenomenon is most likely due to the reduction of the oxygen-containing functional groups and better rGO packing, as reported previously [2]. Unlike in the pure GO films, the films with CNC did not experience a significant increase in tensile strength after reduction. This is due to the structural changes (lack of packing) brough about by the CNC addition, resulting in progressive damage, evident by the reduced slop of the stress-strain curves beyond 0.2% strain.

From previous reports, cross-linkers typically result in a better stress transfer between GO sheets [11, 12]. In this study, the films with higher interfacial interactions did not show better stress transfer, most likely due to sheet slippage and delamination from suboptimal interlayer packing of GO and rGO particles in the CNC-containing films. Hydrogen bonds are initially stretched until broken, and then are reformed [12]. As shown in Figure 2d, it is possible that the hydrogen bonds are not reforming efficiently once films are damaged beyond their elastic limit, except for the rGO ones, due to inefficient packing. This would explain the high elastic modulus but lower strength of the GO-CNC films. In-situ Raman tensile testing can measure strain in rGO and GO to better explain stress-transfer and failure mechanisms better.

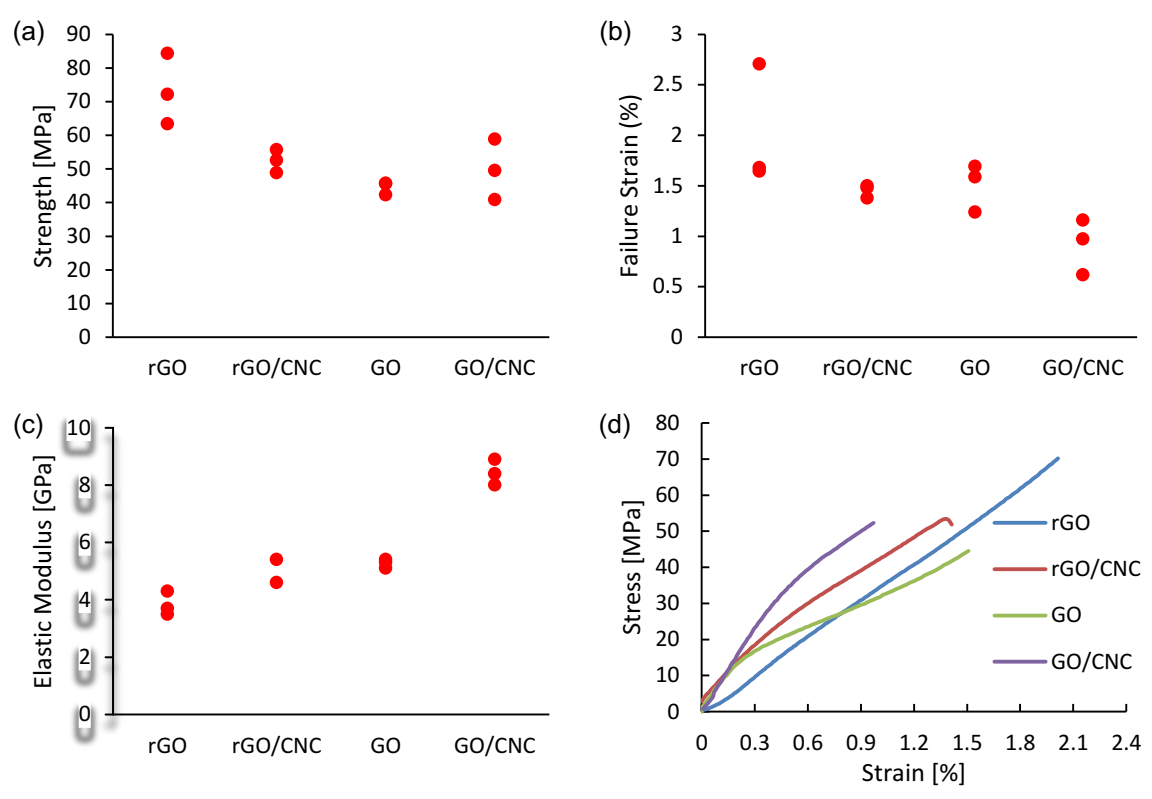


Figure 2. (a) Strength, (b) Failure Strain, (c) Elastic Modulus, and (d) Representative stress-strain curves of GO-based films.

In figure 3(a-d), cross-sectional SEM images of the four samples are shown. The micro-graphs show the multilayered nature of all samples. The topological images of the film can be seen in figure 3(e-h). Both the unreduced films are black in color but become more silver after reduction. This silver color is more apparent in the pure rGO film than the rGO/CNC film.

For graphitic materials, two distinct bands appear in the 1000-2000 cm<sup>-1</sup> Raman shift range. These two bands are the D and G band, where the D band represents disorder in the carbon structure and the G band represents the stretching of the C-C bond in graphitic materials [13, 14]. In graphene oxide, the D band appears at about 1350 cm<sup>-1</sup> and the G band appears at around 1580 cm<sup>-1</sup>. For the insitu Raman spectra captured, the degree of downshift of the G-peak represents C-C bond stretching.

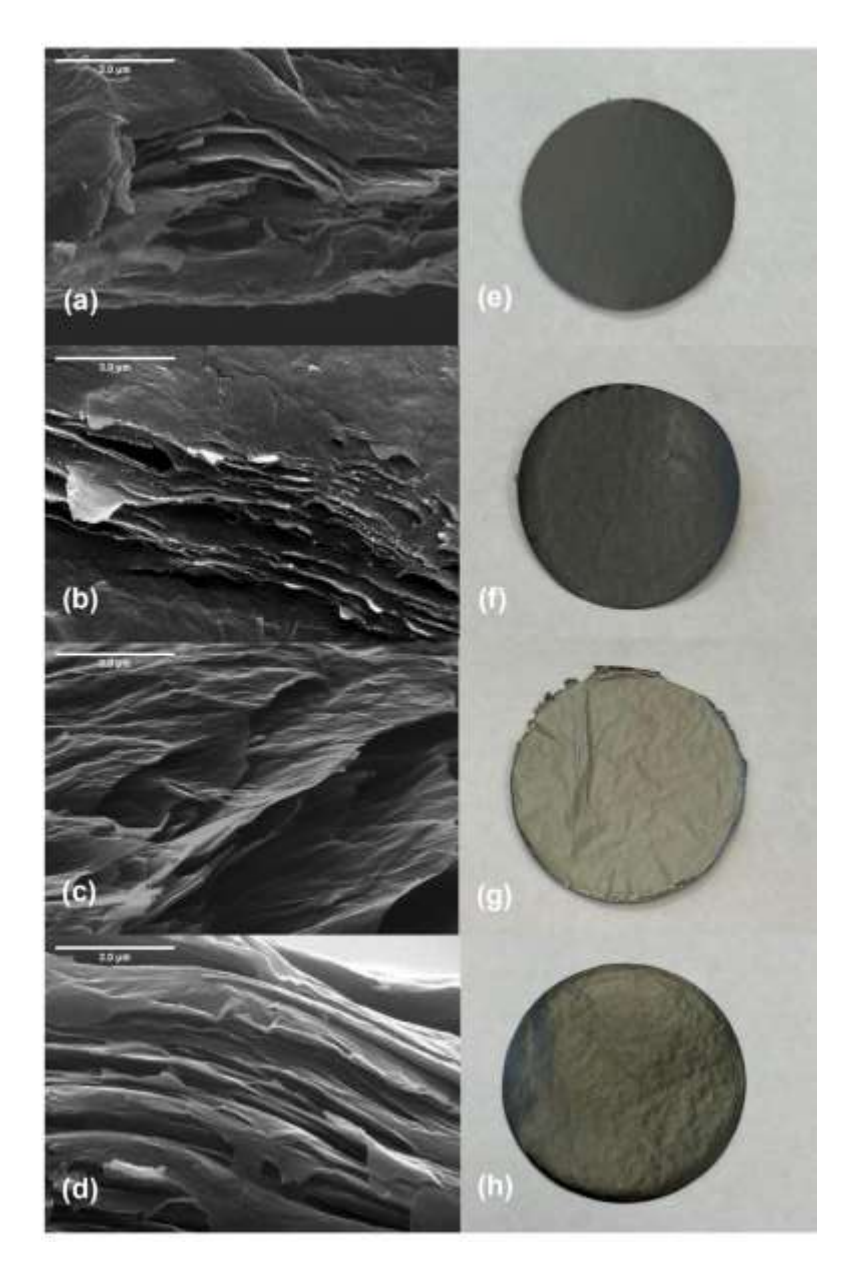


Figure 3. SEM images and Photos of GO and rGO films: (a-d) Cross-sections of pure GO, GO/CNC, pure rGO, and rGO/CNC films, respectively. (e-h) Images of pure GO, GO/CNC, pure rGO, and rGO/CNC films, respectively.

In figure 4, the in-situ Raman spectroscopy data is shown for all four film samples. The D-peak, located at about 1350 cm, and the G-peak, located at about 1580 cm $^{-1}$ , were both prominent in all Raman spectra. The D- and G-Peak are labeled for one spectrum in figure 4(a). This was expected since the films are of semi-ordered graphitic material. The reduction process brings the film structure closer to pure graphene [15], Through reduction, the intensity ratio of the peaks will increase due to change in carbon structure of the GO films, brought on by the removal of both carbon and oxygen groups [2]. For both the GO and GO/CNC films,  $I_D/I_G$  is about 1.1 but slightly increases once reduced.

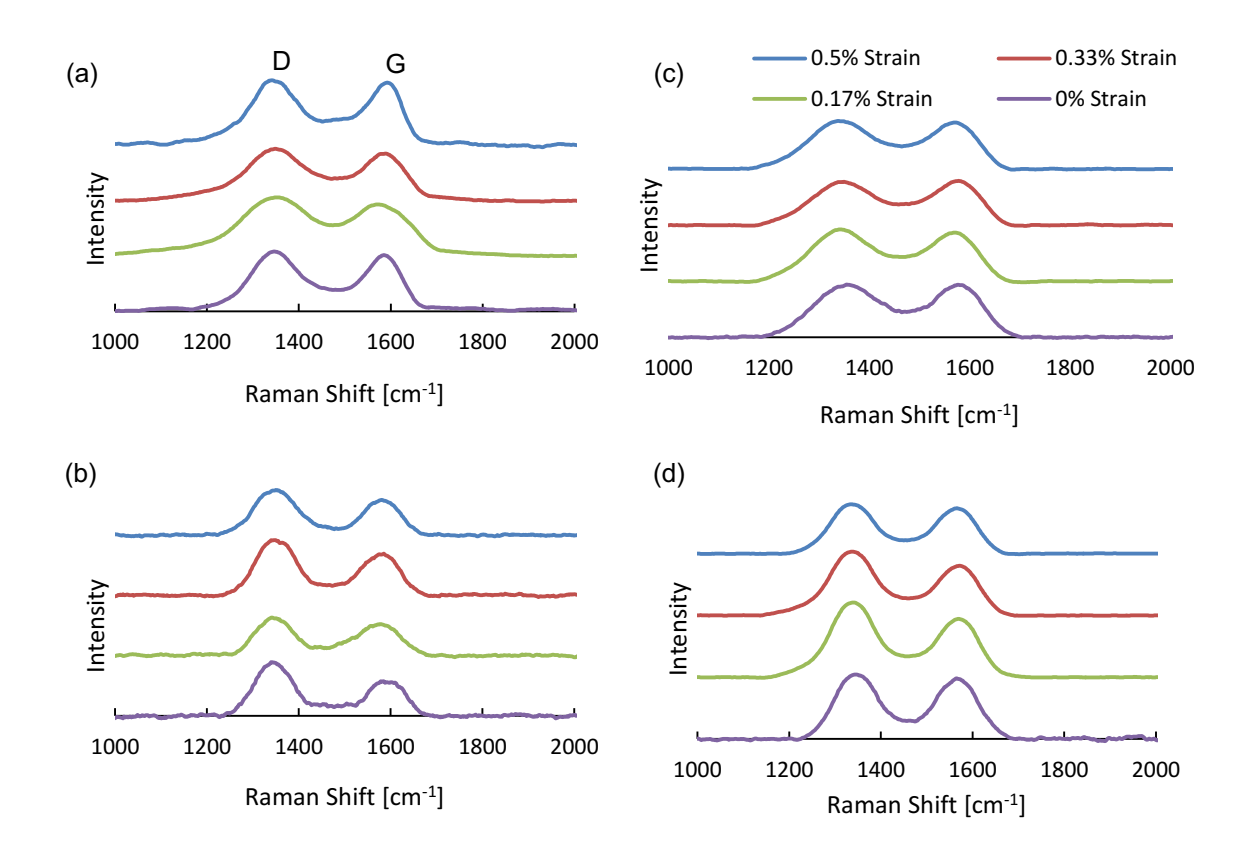


Figure 4. In-Situ Raman Spectroscopy Data. (a) Pure GO film (b) Pure rGO film (c) GO/CNC film (d) rGO/CNC.

Figure 5 show the downshift data of the G-peak from the in-situ Raman spectroscopy study, for a single point in the gauge section up to failure, for the tested samples. The G-peak is highly sensitive to strain, and a downshift in G-peak is expected with increasing strain in GO or rGO particles [9, 13]. Changes in the atomic structure due to strain can be, therefore, observed with changes to the G-peak [16]. More downshift in the G-peak means a more efficient stress transfer to the constituent particles [17]. A lack of substantial downshift means that the stress is not being transferred, indicating inter-sheet slippage [18].

It should be noted that the tensile stresses and strains are averaged over the gauge section, however, the Raman data is only for a single point in the gauge section. Raman data, therefore, exhibit large variations in G-peak downshifts as the GO or rGO particles under the Raman laser stick and slip successively. At 0.17% strain, GO-CNC sample exhibits the highest downshift, i.e., strain in GO particles. This is in agreement with the tensile modulus values, confirming that the combination of abundant functional groups and CNC results in a relatively high stress-transfer between the GO particles. Except for rGO, all samples exhibit small G-peak downshifts over the measured strain range. This is a result of significant sheet-sheet slippage due to inefficient packing. rGO sample exhibits the highest

downshift, commensurate with its highest strength among all samples. Such downshift is a result of a continuous stress transfer between rGO particles up to failure. This relation has also been suggested in the study by Wan et al [17]. From previous studies, it was expected that the addition of stronger interlayer bonds would improve the stress transfer between GO sheets [12, 18]. In the present study, however, the differences in film microstructures played a major role in determining mechanical properties of the films.

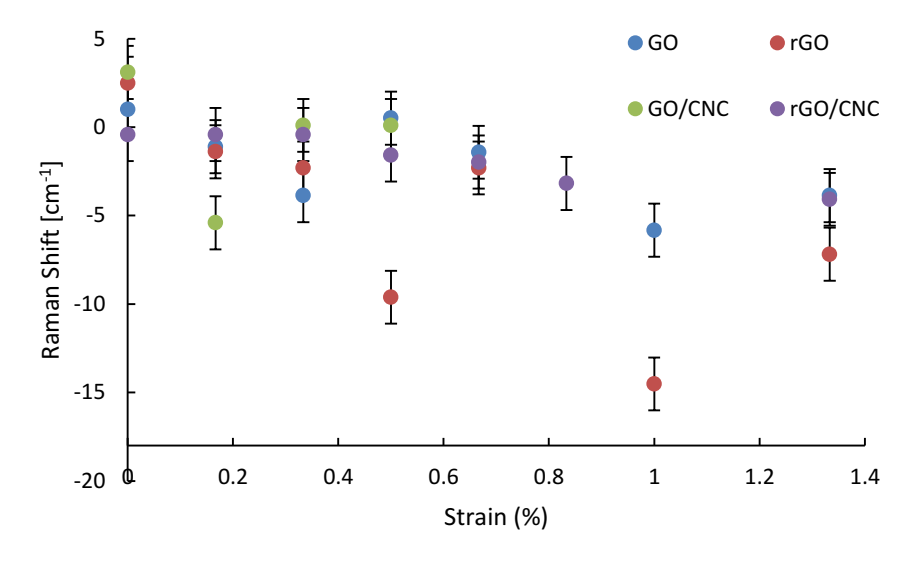


Figure 5. Raman Downshift of the G-Peak.

# **CONCLUSIONS**

This study investigates how interfacial interactions, particle packing, and hydrogen bonds affect stress transfer and failure in of GO and rGO films. The GO-CNC and rGO-CNC films showed the highest elastic modulus but lowest strength and failure strain. In-situ Raman spectra of these two samples, showed efficient stress transfer in the elastic regime, due to CNC interactions with the sheets, but substantial slippage at higher strains due to sheet delamination and damage. It was concluded that both an efficient packing and strong inter-linking is required to achieve stiff and strong GO-based films.

#### **ACKNOWLEDGEMENT**

Authors gratefully acknowledge the support under the NSF CAREER award #CMMI-1847035.

#### **REFERENCES**

- [1] L. Liu, J. Zhang, J. Zhao, and F. Liu, "Mechanical properties of graphene oxides," *Nanoscale*, vol. 4, no. 19, p. 5910, 2012, doi: 10.1039/c2nr31164j.
- [2] S. Pei, J. Zhao, J. Du, W. Ren, and H.-M. Cheng, "Direct reduction of graphene oxide films into highly conductive and flexible graphene films by hydrohalic acids," *Carbon*, vol. 48, no. 15, pp. 4466-4474, 2010/12 2010, doi: 10.1016/j.carbon.2010.08.006.
- [3] C. Cao, M. Daly, C. V. Singh, Y. Sun, and T. Filleter, "High strength measurement of monolayer graphene oxide," *Carbon*, vol. 81, pp. 497-504, 2015/01 2015, doi: 10.1016/j.carbon.2014.09.082.
- [4] V. B. Mohan, R. Brown, K. Jayaraman, and D. Bhattacharyya, "Characterisation of reduced graphene oxide: Effects of reduction variables on electrical conductivity," *Materials Science and Engineering: B*, vol. 193, pp. 49-60, 2015/03 2015, doi: 10.1016/j.mseb.2014.11.002.
- J. Chen, H. Li, L. Zhang, C. Du, T. Fang, and J. Hu, "Direct Reduction of Graphene Oxide/Nanofibrillated Cellulose Composite Film and its Electrical Conductivity Research," (in eng), *Sci Rep*, vol. 10, no. 1, pp. 3124-3124, 2020, doi: 10.1038/s41598-020-59918-z.
- [6] A. Pareek and S. Venkata Mohan, "Graphene and Its Applications in Microbial Electrochemical Technology," in *Microbial Electrochemical Technology*, ed: Elsevier, 2019, pp. 75-97.
- [7] O. C. Compton *et al.*, "Tuning the Mechanical Properties of Graphene Oxide Paper and Its Associated Polymer Nanocomposites by Controlling Cooperative Intersheet Hydrogen Bonding," *ACS Nano*, vol. 6, no. 3, pp. 2008-2019, 2012/02/22 2012, doi: 10.1021/nn202928w.
- [8] Y. Liu, B. Xie, Z. Zhang, Q. Zheng, and Z. Xu, "Mechanical properties of graphene papers," *Journal of the Mechanics and Physics of Solids*, vol. 60, no. 4, pp. 591-605, 2012/04 2012, doi: 10.1016/j.jmps.2012.01.002.
- [9] B. Mohan, G. Freihofer, B. Wirth, and S. Raghavan, "Measuring Tensile Stresses in CNF/Polymer composites using Raman Spectroscopy," presented at the 52nd AIAA/ASME/ASCE/AHS/ASC Structures, Structural Dynamics and Materials Conference, 2011/04/04, 2011. [Online]. Available: http://dx.doi.org/10.2514/6.2011-1791.
- [10] M. S. Dresselhaus, A. Jorio, M. Hofmann, G. Dresselhaus, and R. Saito, "Perspectives on Carbon Nanotubes and Graphene Raman Spectroscopy," *Nano Letters*, vol. 10, no. 3, pp. 751-758, 2010/01/19 2010, doi: 10.1021/nl904286r.
- [11] M. Yang *et al.*, "Interlayer crosslinking to conquer the stress relaxation of graphene laminated materials," *Materials Horizons*, vol. 5, no. 6, pp. 1112-1119, 2018, doi: 10.1039/c8mh00817e.
- [12] N. V. Medhekar, A. Ramasubramaniam, R. S. Ruoff, and V. B. Shenoy, "Hydrogen Bond Networks in Graphene Oxide Composite Paper: Structure and Mechanical Properties," *ACS Nano*, vol. 4, no. 4, pp. 2300-2306, 2010/04/09 2010, doi: 10.1021/nn901934u.
- [13] E. I. Bîru and H. Iovu, "Graphene Nanocomposites Studied by Raman Spectroscopy," in *Raman Spectroscopy*, ed: InTech, 2018.
- [14] K. N. Kudin, B. Ozbas, H. C. Schniepp, R. K. Prud'homme, I. A. Aksay, and R. Car, "Raman Spectra of Graphite Oxide and Functionalized Graphene Sheets," *Nano Letters*, vol. 8, no. 1, pp. 36-41, 2007/12/22 2007, doi: 10.1021/nl071822y.
- [15] W. Liu and G. Speranza, "Tuning the Oxygen Content of Reduced Graphene Oxide and Effects on Its Properties," (in eng), *ACS Omega*, vol. 6, no. 9, pp. 6195-6205, 2021, doi: 10.1021/acsomega.0c05578.
- [16] N. Ferralis, "Probing mechanical properties of graphene with Raman spectroscopy," *Journal of Materials Science*, vol. 45, no. 19, pp. 5135-5149, 2010/06/15 2010, doi: 10.1007/s10853-010-4673-3.
- [17] S. Wan *et al.*, "Sequentially bridged graphene sheets with high strength, toughness, and electrical conductivity," (in eng), *Proc Natl Acad Sci U S A*, vol. 115, no. 21, pp. 5359-5364, 2018, doi: 10.1073/pnas.1719111115.
- [18] L. Cao, Q. Sun, H. Wang, X. Zhang, and H. Shi, "Enhanced stress transfer and thermal properties of polyimide composites with covalent functionalized reduced graphene oxide," *Composites Part A: Applied Science and Manufacturing*, vol. 68, pp. 140-148, 2015/01 2015, doi: 10.1016/j.compositesa.2014.10.007.